# Movement of the tongue during normal breathing in awake healthy humans

S. Cheng, J. E. Butler, S. C. Gandevia and L. E. Bilston

Electromyographic (EMG) activity of the airway muscles suggest that genioglossus is the primary upper airway dilator muscle. However, EMG data do not necessarily translate into tissue motion and most imaging modalities are limited to assessment of the surfaces of the upper airway. In this study, we hypothesized that genioglossus moves rhythmically during the respiratory cycle and that the motion within is inhomogeneous. A 'tagged' magnetic resonance imaging technique was used to characterize respiratory-related tissue motions around the human upper airway in quiet breathing. Motion of airway tissues at different segments of the eupnoeic respiratory cycle was imaged in six adult subjects by triggering the scanner at the end of inspiration. Displacements of the 'tags' were analysed using the harmonic phase method (HARP). Respiratory timing was monitored by a band around the upper abdomen. The genioglossus moved during the respiratory cycle. During expiration, the genioglossus moved posteriorly and during inspiration, it moved anteriorly. The degree of motion varied between subjects. The maximal anteroposterior movement of a point tracked on the genioglossus was $1.02 \pm 0.54$ mm (mean $\pm$ s.d.). The genioglossus moved over the geniohyoid muscle, with minimal movement in other muscles surrounding the airway at the level of the soft palate. Local deformation of the tongue was analysed using two-dimensional strain maps. Across the respiratory cycle, positive strains within genioglossus reached peaks of $17.5 \pm 9.3\%$ and negative strains reached peaks of $-16.3 \pm 9.3\%$ relative to end inspiration. The patterns of strains were consistent with elongation and compression within a constant volume structure. Hence, these data suggest that even during respiration, the tongue behaves as a muscular hydrostat.

The tongue forms a major part of the upper airway and is comprised of both intrinsic and extrinsic muscles. The intrinsic muscles (verticalis, transverse, inferior longitudinal and superior longitudinal) originate and terminate within the tongue, while the extrinsic muscles (genioglossus, styloglossus, geniohyoid and hyoglossus) arise from external structures and insert into it (Takemoto, 2001). The tongue is largely incompressible and has been considered a 'muscular hydrostat' with a constant tissue volume that is redistributed when part of it contracts or is compressed by outside structures (Kier *et al.* 1989; Napadow *et al.* 1999a: for review Gilbert *et al.* 2007). Several studies have examined how this muscle deforms in various physiological tasks, such as speech and swallowing (Napadow *et al.* 1999a,b; Parthasarathy *et al.* 2007). However, little is known about the dynamic internal deformation of the tongue during quiet breathing. During respiration, the tongue must be positioned so that

the airway is patent and many studies have been conducted to investigate airway patency. The two main methods that have been used are measurement of the electromyographic activity (EMG) of the muscles and imaging of the upper airway.

A common assumption is that increased EMG in muscles of the tongue stiffens it and acts to reduce collapsibility of the airway to decrease airway resistance. EMG studies have revealed respiratory related activities in genioglossus (e.g. Sauerland & Harper, 1976; Mathew *et al.* 1982; Mezzanotte *et al.* 1992a; Malhotra *et al.* 2000, 2002), alae nasi (e.g. Strohl *et al.* 1980; Mezzanotte *et al.* 1992b), palatoglossus and tensor palatini (e.g. Tangel *et al.* 1995; Malhotra *et al.* 2000). EMG studies of the genioglossus have suggested that this muscle dilates the upper airway during inspiration as the onset of the activity is just before airflow (Strohl *et al.* 1980; Hudgel *et al.* 1993). Negative pressure in the upper airway appears to activate this muscle reflexly as there is a robust correlation between negative epiglottic pressure and the level of genioglossus EMG (Mathew *et al.* 1982; Horner *et al.* 1991; Berry *et al.* 2003).

This paper has online supplemental material.

However, genioglossus is also activated by descending respiratory drive even in the absence of negative pressure (Innes *et al.* 1995; Pillar *et al.* 2001). Nevertheless, since EMG does not necessarily translate into muscle motion, the exact mechanism by which the airway is kept patent by genioglossus is unknown.

Many imaging modalities have been used to assess airway patency directly. These include endoscopic imaging (e.g. Morrell & Badr, 1998; Kuna, 2004), X-ray fluoroscopy (e.g. Wheatley *et al.* 1991), acoustic reflection (Brown *et al.* 1986), computer tomographic imaging (CT scans, e.g. Schwab *et al.* 1993), magnetic resonance imaging (MRI, e.g. Trudo *et al.* 1998), and optical coherence tomography (OCT; Armstrong *et al.* 2006). Many studies have analysed the geometry and structure of the airways from images derived from X-rays, CT scans and MRI. This is possible because of the high contrast between the airway and the adjacent tissues. However, studying the changes in airway size and shape alone gives limited information on how airway muscles could have deformed to produce those changes. In addition, due to the low temporal resolution of many imaging techniques, they are ill-suited to measuring dynamic deformation of the upper airway tissues during breathing. Methods such as endoscopic imaging, video fluoroscopy and OCT are limited to the assessment of the external surface of the tongue and other airway muscles.

MRI tagging (e.g. Prince & McVeigh, 1992) is a relatively new imaging technique that has been used to quantify the physiological deformations of the lung, heart and tongue (e.g. Napadow *et al.* 1999*a*, 2001; Osman *et al.* 2000). This method works by spatial modulation of the longitudinal magnetization of the subject's tissue using the MR scanner to create temporary features within the tissues known as tags. A fast spoiled gradient echo imaging technique is then used to reveal how these tags deform with tissue motion (Osman *et al.* 1999). This method has also been used to investigate tongue motion due to the simulation of the medial hypoglossal nerve in rats (Brennick *et al.* 2004). In the current study, we aimed to use MRI tagging of the human upper airway to determine whether there is respiratory-related tissue motion in quiet breathing, which tissues have the largest movement, and how any motion is distributed. We hypothesized that genioglossus moves rhythmically during the respiratory cycle and that the motion within is inhomogeneous. This is an essential study to understand how airway muscles help to keep the airway patent during respiration and how this behaviour may change under pathological conditions. Although the movement of the airway muscles may change from wakefulness to sleep (e.g. Worsnop *et al.* 1998, 2000) and also may differ between healthy subjects and sleep apnoea patients, the basic physiology of how they keep the airway patent during normal breathing in awake humans needs to be determined. A preliminary version of this work has been presented (Cheng *et al.* 2007).

## Methods

Six normal subjects (4 females and 2 males) volunteered for this study. None had a history of a major respiratory or sleep disorder. The mean age of the subjects was $25 \pm 3$ years (mean $\pm$ s.d.) and the mean body mass index (BMI) was $20.27 \pm 1.4$ kg m$^{-2}$ (mean $\pm$ s.d.) with a range from 19.1 to 22.7 kg m$^{-2}$. Approval for this study was granted by the Human Research Ethics Committee of the University of New South Wales. The study was conducted according to the *Declaration of Helsinki* and informed written consent was obtained. All subjects had no contra-indication for MR imaging.

### Procedures prior to scan

The resting ventilation of each subject was monitored while supine to ensure that consistent breathing would be achieved in the MR environment. This was done with a MR-compatible respiratory band made from an adjustable elastic band incorporating an air pillow connected via a stiff tube to a remote pressure transducer (Validyne, Northridge, CA, USA). A real-time digital oscilloscope (Tektronix, TDS 210, Oregon, USA) was used to monitor the pressure in the air pillow. The respiratory band was placed around the abdomen about 20 mm below the lower margin of the rib cage (Fig. 1*A*).

The effectiveness of the respiratory band in monitoring respiration was checked by measuring air flow at the mouth during quiet breathing on a mouthpiece outside the scanner in the laboratory. Airflow was measured with a pneumotachometer (model 3700A, Hans Rudolph Inc., Kansas City, MO, USA) and the airflow signal was integrated to give volume. The flow, volume and respiratory band pressure signals were digitized at 1000 Hz and recorded directly onto a computer (Fig. 1*C*).

During the preparatory studies, subjects lay supine with their head in a similar headcoil to that in the MR scanner. Since flexion or extension of the head alters upper airway size (Amis *et al.* 1999), the head was placed in the neutral position. This was defined by aligning the Frankfort plane, a plane from the orbit of the eye to the superior portion of the tragus, perpendicular to the scanner table (Trudo *et al.* 1998). Subjects were requested to relax and breathe quietly through the nose. The respiration of each subject was then monitored in the scanner with the respiratory band but without the mouthpiece. Subjects remained awake throughout the studies.

### Scanning protocol

A 3T MR scanner (Philips) was used. Subjects (with the respiratory band) were placed on the scanner bed and asked to keep still and breathe quietly. Pads were placed around their head to minimize head motion. We constantly communicated with subjects to ensure that they

were awake during scanning and this was checked by verbal report after all scanning sessions. The tagging technique is normally cardiac gated and the sequence requires a cardiac pulse. In this study, MR scanner was triggered by a transistor–transistor logic (TTL) pulse sequence generated by a program created using LabVIEW v8.2 (National Instruments Corp., Austin, TX, USA). A data acquisition card (VI6008, National Instruments) was used to send the output signal to the vector cardiogram input of the scanner. Although only a single TTL pulse triggers
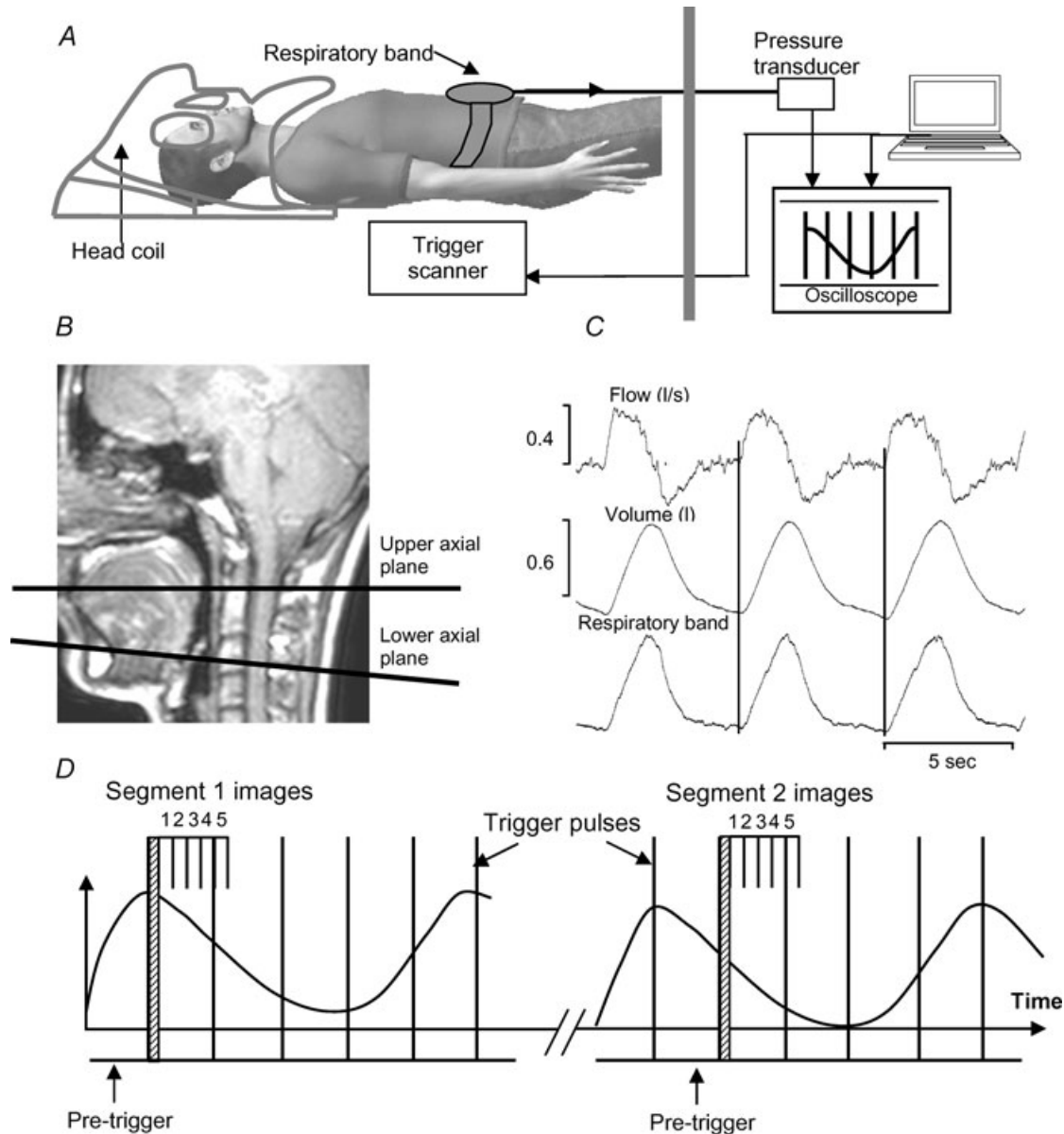


**Figure 1. Equipment, imaging planes and effectiveness of respiratory band**
*A*, subject in a head coil. A respiratory band is fixed around the upper abdomen by an adjustable band and is connected to a pressure transducer. Regular trigger pulses are generated using a computer. Both the pressure and trigger pulses are displayed on the same oscilloscope. The trigger pulses are also connected to the scanner. The oscilloscope shows a respiratory cycle divided into 5 equal segments by 6 trigger pulses. *B*, a T2-weighted image of the head in the mid-sagittal plane. The locations of the 2 axial planes were determined from the sagittal image as shown. The upper axial plane touched the tip of the soft palate and the lower axial plane touched the caudal end of the epiglottis and was positioned parallel to the mandible. *C*, typical relation between the pressure from the respiratory band and airflow measured at the mouth. The two vertical lines show coincidence of the airflow, volume and pressure from the respiratory band at the onset of inspiration. *D*, an example of how data are acquired for the 1st and 2nd segment of the respiratory cycle. After 'pretriggering', the acquisition of the 5 images is not immediate, but starts at the next trigger pulse. The shaded bar represents the time delay due to the laying down of tags (∼140 ms; see Methods). For both segments shown diagrammatically here, the beginning and end of the cycle, as indicated by the inspiratory peak, align with the pulses (6 pulses per breath), so the data are accepted for analysis.

the scanner, the tagging protocol requires initialization by detecting periodic TTL pulses. After triggering, the scan was preceded by tagging pulses which saturated the longitudinal magnetization of the tissues (CSPAMM). This took ~140 ms and resulted in a square rectilinear grid formed by horizontal and vertical dark-coloured tagged lines on the tissue. The subsequent tagged images of the scan show the tissue movements according to grid deformation. The number of tagged images in a scan sequence can be preset.

One drawback of the tagging technique is that tags fade with time. Preliminary studies showed that tag fading occurred after the 4th image, and thus only four to five tag images were used in each scan. Since each tagged image took about 230 ms to acquire, the effective time for each scan was ~1 s. Therefore, multiple scans were needed to capture airway muscle movements throughout the respiratory cycle. This was achieved by generating a unique pulse train for every individual. The frequency of the pulse train was assigned in such a way that the respiratory cycle was covered by a specified number of pulses. The pulse train and the pressure from the respiratory band were viewed on an oscilloscope. By ensuring that the first and the last pulse fell on successive inspiratory peaks (before expiration commenced), scans of different segments of the respiratory cycle were achieved. Thus, each segment consisted of four to five tagged images and the first image had the undeformed tagged lines. A respiratory cycle that is divided into four segments therefore had a total of 16–20 tagged images. In this study, three independent scans were performed for each segment of the respiratory cycle to show that the results were reproducible.

Images were taken in a mid-sagittal plane and two axial planes. The upper axial plane was defined by the tip of the soft palate as observed in the sagittal plane and the lower axial plane was defined by the caudal end of the epiglottis and was positioned in such a way that it was parallel to the mandible (Fig. 1*B*). The upper axial plane was chosen to determine the tissue motion in the region of the soft palate. The lower axial plane was chosen because preliminary studies showed that genioglossus moved parallel to the mandible. Other imaging parameters were: field of view 22 cm; flip angle 90 deg; spin echo repetition time 400 ms; echo time 16 ms; $256 \times 256$ matrix and tag spacing 8.6 mm with a slice thickness of 10 mm.

## Analysis

Tracking of the tags during tissue deformation was performed with the harmonic phase method (HARP). This uses the principle that tissue deformation is directly related to the locations of the spectral peaks found in the tagged MR data in the Fourier domain since changes in tag spacing alter the spatial frequency of the tagged grid.

Further details of the HARP method are available (Osman *et al.* 1999). Tracking of tissue motion was performed by first defining the coordinates of the points of interest on the undeformed tagged image of the first segment. The new locations of the points in subsequent deformed tagged images were analysed by HARP. To ensure that the same anatomical location is tracked throughout the respiratory cycle, the average of the *x,y* coordinates of the tracked point from the last frame of the three repetitions of the previous segment were used as the starting coordinates for that point in the next segment. On the mid-sagittal tagged images, a point on the genioglossus was tracked at a distance of ~10 mm anterior to the epiglottis (point A, Fig. 2*A*). Another point was tracked on the centre of the geniohyoid (point B, Fig. 2*A*). On the tagged images of the upper axial plane, a point was tracked posterior (point C) and lateral (point D) at ~10 mm away from the airway. Tracking of points started from the end of inspiration. This was done because this timing was more stable and predictable than the onset of inspiration.

To show the regional movements within the tongue during the respiratory cycle, a grid of points was tracked in the mid-sagittal and lower axial plane. Deformation of a flexible body is quantitatively characterized by the strain, which represents the deformation of a region of tissue relative to its initial size. Elongation is indicated by a positive strain, and compression or shortening by a negative strain. The strain of the tongue was calculated from the grid. This was performed by first creating a triangular mesh of the tongue using the points as vertices for the mesh. The same triangular mesh pattern was then applied to the corresponding intersections in the deformed image. The right angle sides of each triangular element were composed of a horizontal and vertical line element. Strains were computed based on the changing length of these elements (Napadow *et al.* 1999*a*). This is achieved by determining the deformation gradient tensor, *F*, which represents the transformation of the undeformed line segment to the deformed line segment. The 2D Lagrangian strain tensor, *E*, of each triangular element is related to the deformation gradient by the following formula. *I* is an identity matrix.

$$E = (F^T F - I/2)$$
$$I = \begin{bmatrix} 1 & 0 \\ 0 & 1 \end{bmatrix}$$

The strain maps were smoothed with bicubic spline surfaces and superimposed on the tagged images. Both generation of the mesh and analysis of the strain were implemented using MATLAB (v 7, The MathWorks, Natick, MA, USA). All strains are calculated relative to a nominal undeformed state at the end of inspiration, at which time point there are potentially non-zero tissue loads. Note that the reported strains are thus

relative values, and do not necessarily reflect muscle contraction or elongation *per se*, but rather the combined effect of muscle activity and other pressures and forces acting on the tissue relative to its position at end-inspiration.

## Statistical analysis

Data for the movement of four specific points in the upper airway were compared using a one-way repeated measures analysis of variance (with Tukey's *post hoc* test). Correlations between the magnitude of movement of the point on genioglossus and the subjects' breathing period, body mass index, and airway cross-sectional areas were evaluated with Spearman's rank correlation. Statistical significance was set at 5%. All data are presented as means ± s.d. in the text.

## Results

### Respiratory monitoring

Figure 1*C* shows typical raw data obtained from a subject during quiet breathing in the laboratory. The pressure change in the abdominal band closely followed the lung volume signal derived from airflow at the mouth. During scanning, duration of the expiratory phase was $51 \pm 7.1\%$ of the total respiratory cycle (mean ± s.d.). The maximal time delay between airflow and pressure measured from the respiratory band is < 100 ms.

### Dynamic images (movie files) of the tongue movement during the respiratory cycle

Tagged images obtained from the same imaging planes were compiled to produce movie files, five of which are
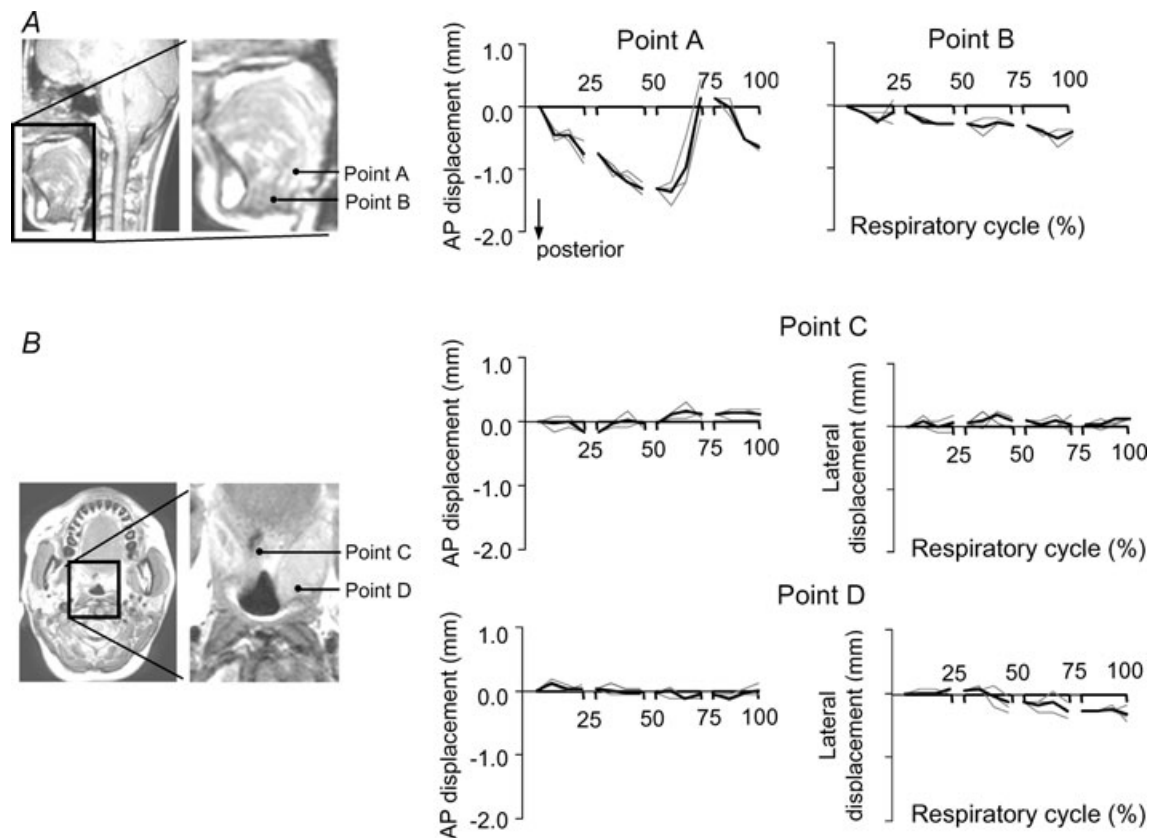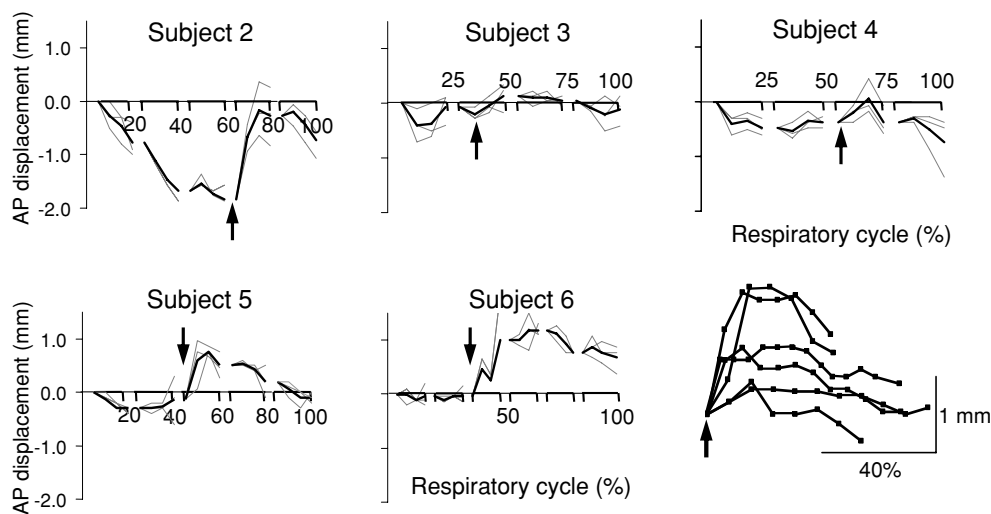


**Figure 2. Displacements of tissue during the respiratory cycle in subject 1**
*A*, average anteroposterior motion of point A and point B tracked on the genioglossus and the geniohyoid, respectively, starting from expiration (end inspiration). At the left are anatomical images from the subject on which the positions of points A–D are marked. The posterior and anterior motions of the points are represented by negative and positive displacements, respectively. *B*, average motion of 2 points tracked above (point C) and adjacent (point D) to the airway in the upper axial plane. For point C, the posterior and anterior motions are represented by negative and positive displacements, respectively. For point D, motion towards the left and right is represented by negative and positive displacements, respectively. Motions of the points are analysed 3 times for each segment of the respiratory cycle and the results are shown by the lines in grey. The mean results are shown by the black lines. The gaps between each respiratory segment are included to indicate that data for different segments are collected from different breaths. The respiratory cycle begins at the end of inspiration.

presented as online supplemental material. Three files from one subject (subject 1) show the deformation of the tongue during respiration starting from the onset of expiration (see also Fig. 2). One file is shown for each imaging plane; mid-sagittal, upper axial and lower axial (see supplemental material). As the respiratory cycle of this subject was subdivided into four segments, each movie was compiled from four sequences of tagged images, one from each segment. In the mid-sagittal plane, genioglossus was defined by an enclosed region formed by a yellow marker ellipse (Movie 1, Sagittal). At the start of each segment, an undeformed tag pattern was reapplied so that tag bending in movie files is relative to tag positions at the start of that segment and not relative to end inspiration. In Movie 1, bending of the vertical tag lines within the marker ellipse during the respiratory cycle is obvious. The bending pattern signifies how genioglossus deforms during respiration. During expiration, the genioglossus moved posteriorly and this was revealed in two consecutive respiratory segments. During the early phase of inspiration, genioglossus moved anteriorly. The muscle moved posteriorly again towards the end of inspiration. There was little deformation of the tag lines outside the marker ellipse, and thus respiratory movement of adjacent muscles and tissues was small. The anterior movement of the genioglossus during inspiration for the remaining five subjects can be observed in Movie 5 (Sagittal-all).

Corresponding observations can be made from the movie files produced from the other two imaging planes. In the upper axial plane (Movie 2, Upperaxial), tag movements were minimal at the level of the soft palate, indicating that there were only small movements in other muscles surrounding the upper airway at this level. In the lower axial plane (Movie 3, Loweraxial), deformation of the tags anterior to the airway (genioglossus) was observed. Genioglossus moved posteriorly in expiration in two consecutive segments and the airway aperture reduced in size. During inspiration, the genioglossus moved anteriorly back towards its initial position and opened the airway in that plane. Although similar observations were made in all the subjects, genioglossus movement was small in two subjects.

The data also showed that genioglossus appeared to move over the geniohyoid during inspiration. Movie 4 (Sagittal2) is a movie from subject 5 during early inspiration in the mid-sagittal plane (see also Fig. 3). A yellow line aligned approximately parallel to the lower mandible was superimposed on the movie to differentiate genioglossus and geniohyoid. Similar observations to those from subject 1 were made. Bending of the vertical tag lines showed that genioglossus moved anteriorly during inspiration. The tags deformed above and along the superimposed line. Tags below the line showed no deformation and this suggests that the geniohyoid deforms little during inspiration.



**Figure 3. Displacement of tissue during the respiratory cycle for the remaining subjects**
Data shown is for the analysis in Fig. 2*A*. The average motion of point A on the genioglossus starting from end-inspiration for the 5 additional subjects. The respiratory cycle was divided into 6 segments in subject 6, 5 segments in subjects 2 and 5, and 4 segments in subjects 3 and 4. The posterior and anterior motions of the point are represented by negative and positive displacements, respectively. Vertical arrows depict the approximate onset of anterior motion in each subject. The bottom right panel shows mean data superimposed from each subject. The traces are aligned with the onset of apparent anterior motion of genioglossus (vertical arrow) and the gaps between recording segments have been removed. For this panel, data are shown for all subjects and the calibrations are ~1 mm and ~40% of the respiratory cycle.

**Table 1. Average peak-to-peak displacements of points A, B, C and D during the respiratory cycle**

| Upper airway location | Average displacement | |
|---|---|---|
| | Antero-posterior (mm) | Lateral (mm) |
| Point A | 1.02 ± 0.54 | — |
| Point B | 0.34 ± 0.47 | — |
| Point C | 0.14 ± 0.10 | 0.19 ± 0.18 |
| Point D | 0.09 ± 0.08 | 0.13 ± 0.08 |

This shows the average displacement (mean ± s.d.) of points A, B, C and D from end expiration to mid inspiration for 6 subjects. Points A and B are located on the genioglossus and geniohyoid, respectively, in the mid-sagittal plane. Points C and D are located anterior and lateral to the airway, respectively, in the upper axial plane. Movement of points B, C and D was small compared to the movement of Point A.

## Magnitude of tongue displacements during the respiratory cycle

Points were tracked at two locations in the sagittal plane and at two locations in the upper axial plane for subject 1. The displacement of each of these points during the respiratory cycle is shown in Fig. 2. The displacement of point A in genioglossus is greater than the displacement of point B in the geniohyoid (Fig. 2*A*). It is also ∼8 times greater than the displacement of two points (C and D) tracked anterior and lateral to the airway (Fig. 2*B*). To indicate that the data were collected from different breaths (see Methods), the data segments have not been joined along the time axis. Data from each breath and the mean values in each segment of the breath are plotted as grey and black lines, respectively.

The average displacement of point A for the rest of the subjects (2–6) is shown in Fig. 3. The characteristics of genioglossus displacement were similar in subjects 1 and 2. Apart from subject 6, all subjects showed an initial but variable posterior movement of the point tracked on the genioglossus in early expiration. The inspiratory movement of the genioglossus differed among subjects. In subjects 2 and 4, genioglossus moved anteriorly to return to the initial reference position. However, in the rest of the subjects, the genioglossus moved past the reference position during inspiration before it moved back posteriorly. Subjects 3 and 4 had the smallest displacement during respiration. The average peak-to-peak movements of all tracked points for the six subjects are shown in Table 1. The mean maximal displacement of point A for the six subjects was 1.02 ± 0.54 mm (mean ± s.d.). The size of the movements differed for the four points ($P < 0.002$) and movement of point A was significantly greater than that of the other points ($P < 0.03$). It is important to understand that given the arbitrary selection of point A in the genioglossus, it may be that nearby points moved more

than shown in Figs 2 and 3. No significant correlations were observed between the peak-to-peak movement of point A and the duration of the subject's respiratory cycle, body mass index or cross-sectional area of the airway (in either the upper or the lower axial plane).

## Tongue deformation during respiration

The next analysis focused on the magnitude and pattern of tongue deformation in the mid-sagittal plane and lower axial plane. Figure 4 shows the respiratory movement in different regions of the tongue in subject 1. Figure 4*A* and *B* show the location of a grid of points at different phases of the respiratory cycle in the mid-sagittal plane and lower axial plane, respectively. In Fig. 4*B*, all the points were tracked above and along the width of the airway. Tissue in the posterior part of the tongue moved more than the anterior part in the mid-sagittal plane. However, the maximal size and direction of the tissue movement was consistent within some tongue regions. For example, in panel *A*, points in the middle of the 1st, 2nd and 3rd columns that are closest to the airway all moved posteriorly by ∼2 mm at end expiration. In Fig. 4*B*, all the points in the two lower rows of points closest to the airway also moved posteriorly by ∼2 mm at end expiration. Interestingly, in this panel, all the points move distinctly in the anteroposterior direction. Such movements are consistent anatomically with the regional orientation of genioglossus muscle fibres. Similar movements were observed in subjects 2, 5 and 6.

From the data on local movements, the pattern of strain within the genioglossus and adjacent tissues was derived. The deformed grids and calculated strains of the tongue during respiration are shown for the mid-sagittal plane (Fig. 5) and lower axial plane (Fig. 6) for subject 1. Positive strains (elongation) are shown in red and negative strains (compression or shortening) in blue. During expiration, strain increases in the anteroposterior direction in the lower half of the tongue (genioglossus) as it moves posteriorly. The strain is ∼5% at the end of expiration, indicating that it is 5% longer in this direction than at end-inspiration. During inspiration, the genioglossus moves forward and at mid inspiration, muscle fibres have shortened (see arrow in Fig. 5), resulting in negative (compressive) strains in this localized region of ∼20% in the anteroposterior direction. This is accompanied by elongation in the perpendicular (rostro-caudal) direction at the same location, with rostrocaudal shortening of tissues above and below. The magnitude and location of anteroposterior shortening (negative strain) at the centre of genioglossus during inspiration varied between subjects. The positive and negative strains in the muscle reached peaks of 17.5 ± 9.3% and −16.3 ± 9.3%, respectively. Throughout the respiratory cycle, little strain

was observed in the anteroposterior direction in the region of geniohyoid. The strain maps of the lower axial plane commonly showed left–right asymmetry (Fig. 6).

## Discussion

The primary aim of this work was to investigate movement of the tongue during quiet respiration. We studied movements of genioglossus and nearby tissues in awake normal subjects during eupnoea. The results show that apart from the genioglossus, little respiratory movement occurs in the tissues surrounding the airway. This provides strong support for the hypothesis that genioglossus is the primary active dilator of the upper airway in quiet breathing while lying supine awake. Although the size of the genioglossus movement varies across subjects, displacement of genioglossus is linked to the respiratory cycle. During inspiration, the lower part of the genioglossus moves anteriorly. The direction of the tissue movement has a strong anteroposterior component along the direction of genioglossus fibres. In addition, the genioglossus appears to move over the geniohyoid. Although the maps of local strain varied between subjects, their pattern of deformation is consistent with the suggestion that the tongue is a muscular hydrostat

(Gilbert *et al.* 2007). First, the shortening of tissues in a given direction is always accompanied by the elongation of tissues nearby. Secondly, the bidirectional shortening of tissues in the same plane is accompanied by the elongation of tissue at a similar region in the out-of-plane direction. This effect may account for the asymmetry in the axial strain maps. Together with slight angulation of the axial slice plane relative to tongue position, there may also be regional inhomogeneities in muscle activation (Fogel *et al.* 2003; Saboisky *et al.* 2006).

In the present study, one technical difficulty was to ensure that the scan was performed at the right phase of the respiratory cycle. The respiratory frequency of the subjects studied was consistent and we accepted scan data only when the scanner was triggered by a pulse that fell within a pulse train in which the first and the last pulse coincided with two successive inspiratory peaks measured with the respiratory band. However, the timing is subject to error as coincidence of the pulse and the peak of inspiration was judged online. However, the error is likely to be only ∼0.1–0.2 s. Although the data were collected from cycles of similar frequency, the exact expiratory and inspiratory times and tidal volumes were not controlled and vary slightly in normal breathing (e.g. Tobin *et al.* 1983). Moreover, subjects become restless due to long scan



○ End inspiration　▲ End expiration
■ Mid expiration　◆ Mid inspiration
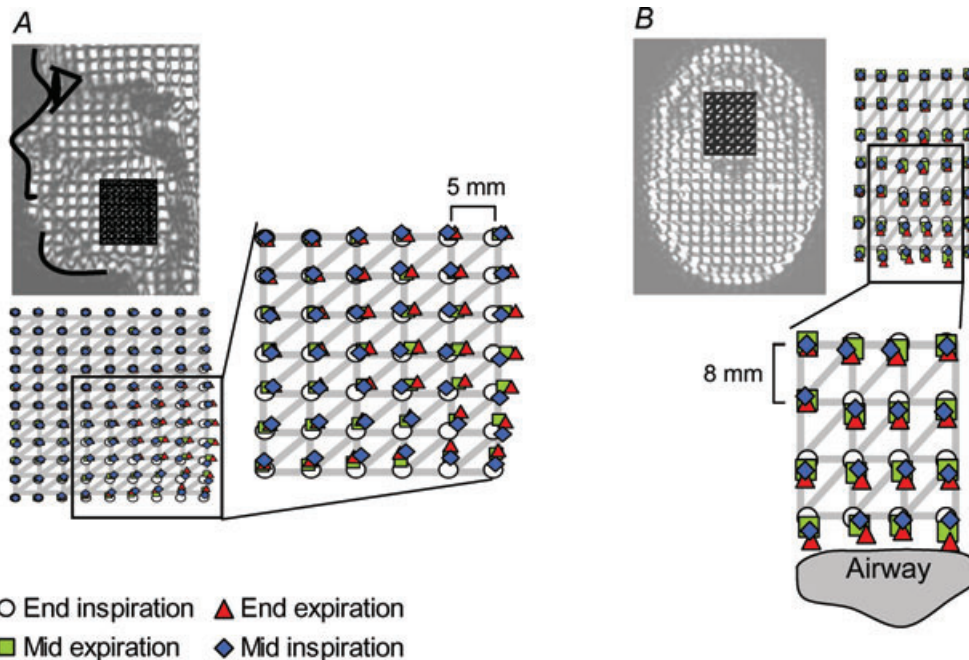
**Figure 4. Movement of a grid of points on the tongue at four times in the respiratory cycle in one subject**
While Fig. 3 and part of Fig. 2*A* show the displacement of a single point tracked on the genioglossus, this analysis shows a grid of points tracked on the tongue. Panels *A* and *B* each show a triangular mesh superimposed on the tagged image in the mid-sagittal plane and lower axial plane, respectively. The vertical and horizontal distance between grid points is 5 mm (panel *A*) and 8 mm (panel *B*). In each panel, the region of the tongue with distinct respiratory movements is enlarged. In both panels, there is movement of the posterior region of genioglossus.

times and this increases the variability in their breathing pattern. The average tolerable scan for each subject lasted ∼45 min. The results of genioglossus motion from point tracking show that there is an apparent 'drift' where the displacements do not always come back to zero. We believe that this is caused by breath-to-breath variability and possibly slight errors in locating exact anatomical points from segment to segment. In addition, like any MR imaging protocol, the tagging data are reconstructed by averaging across the slice. Although we have used an image slice thickness of 10 mm, this averaging should have little effect in our results, especially on images in the mid-sagittal plane. This is because the movement of regions across the width of the airway is rather uniform (Fig. 4B). Lastly, as we have used upper abdominal motion to determine the timing of the respiratory cycle, there may be slight timing differences between pressure in the upper airway and abdominal motion as there are several mechanical steps from the inspiratory pump muscle contraction to airflow in the upper airway. However, our preliminary studies have shown that the pressure signal

from our respiratory bag corresponds very well with the airflow measured at the mouth, i.e. with minimal delay (< 100 ms).

Previous studies using direct muscle stimulation or stimulation of the hypoglossus nerve in rats have reported that genioglossus activation dilates the pharynx (e.g. Brennick et al. 2001, 2007; Fregosi, 2008). The EMG in genioglossus during respiration is driven by a combination of central and reflex drives. Multiunit genioglossus EMG increases in inspiration but maintains a tonic level during expiration (e.g. Sauerland & Harper, 1976; Mathew et al. 1982; Malhotra et al. 2000; Eastwood et al. 2003). Single motor unit studies confirm these findings (e.g. Saboisky et al. 2006, 2007). The phasic inspiratory activity of the genioglossus begins at ∼250 ms prior to inspiratory airflow (e.g. Pillar et al. 2001; Saboisky et al. 2006, 2007) and phasic motor units continue to be recruited throughout the first half of inspiration (Saboisky et al. 2006, 2007). Results from our study suggest that genioglossus probably moves at the time when EMG is increasing during inspiration. However, due to the imprecise timing of the
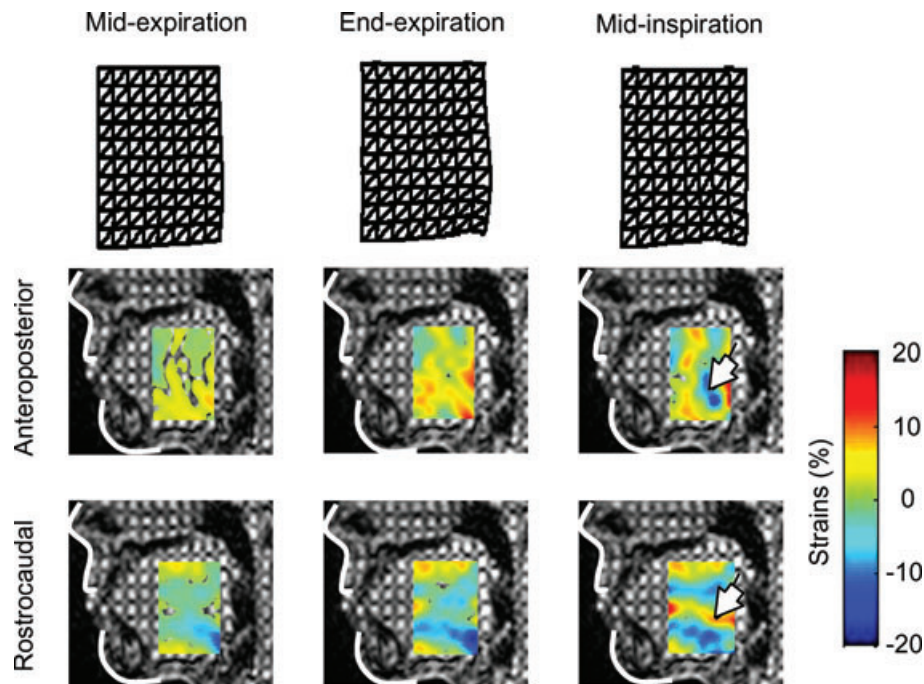


**Figure 5. Direction-dependent strain fields of the tongue in the midsagittal plane during respiration**
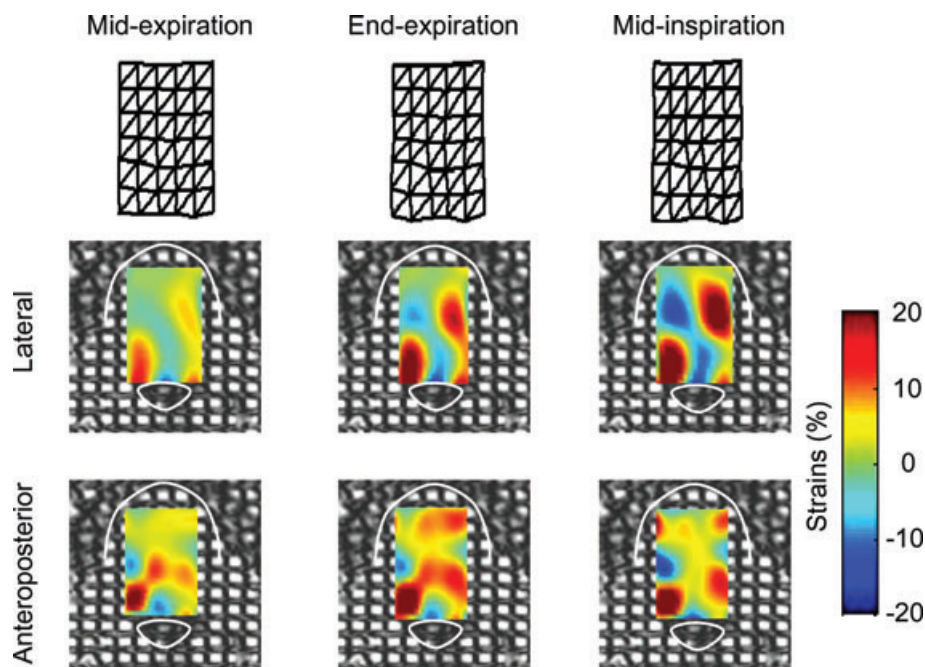This shows deformed grids and strain maps at different times during the respiratory cycle, superimposed on the tongue in the mid-sagittal plane. The three time points were selected based on data acquired from specific respiratory segments in one subject (see Methods). Strain values are represented by the colour bar shown on the right. Tissue was taken to have zero strain at end-inspiration. Red represents positive strain (tissue elongation) of 20% and blue represents negative strain (tissue shortening) of −20%. The middle row of images shows tissue strains in the anteroposterior direction and the lower row of images represents tissue strain in the rostrocaudal direction. Narrower grid spacing in either the anteroposterior or rostrocaudal direction translates into compressive strain in that direction. Note that during mid-inspiration, there is focal shortening of muscle fibres at the posterior region of the genioglossus in the anteroposterior direction (see arrow). This is accompanied by elongation in the same region in the rostrocaudal direction and surrounding regions of tissue shortening above and below (see lower right panel).

scans in relation to the onset of inspiratory airflow, it was not possible to determine if the movement of the genioglossus also begins before inspiratory airflow.

The findings here complement the study of Pillar *et al.* (2001) who reported a correlation between the increase in EMG in the genioglossus and negative epiglottic pressure. The anterior movement of genioglossus would act to resist the effects of the negative inspiratory pressure at the level of the epiglottis. However, we did not detect further anterior movement of genioglossus during the remainder of the respiratory cycle despite the recruitment of some motor units in expiration and expiratory increase in the firing of some tonically firing units (Saboisky *et al.* 2007). This activity presumably stiffens genioglossus but this change in mechanical behaviour could not be measured with the method used in this study. Similar explanations could also be applied to other muscles of the airway such as the tensor palatini, the stylopharyngeal muscles and the intrinsic muscles (Bailey *et al.* 2006). It is likely that these muscles, particularly tensor palatini (e.g. Fogel *et al.* 2003; Pierce *et al.* 2007), receive both respiratory and tonic neural drive, but the level of activity may not be sufficient to produce detectable movement, at least by comparison with that seen in genioglossus. In this study, although genioglossus moves little in subjects 3 and 4, it is also likely that their

airway patencies are protected by stiffening of the muscle. This suggests that the mechanisms which help protect airway patency on a breath-by-breath basis vary between individuals. There was no apparent relationship between the degree of genioglossus motion in an individual and airway cross-sectional area (data not shown). In addition, this study has also confirmed that the geniohyoid showed insignificant movement during the respiratory cycle (see also Yokoba *et al.* 2003). The practical effect of this muscle on airway dilatation during eupnoea is small.

Schwab *et al.* (1993) measured the size of the human upper airway using CT scans and reported an increase in airway size during expiration. They suggested that the increase in airway size was largely due to changes in the lateral dimensions of the airway. The upper axial plane in the current study is the closest to the lower retropalatal plane used by Schwab and colleagues, although the angulation of the slices appears to be somewhat different. We found little movement of the genioglossus or lateral walls in this plane. However, our study cannot directly measure changes in airway area as the boundaries of the airway lumen are obscured by the tags, so it is not possible to directly compare these studies. It may be that the differences in imaging planes account for some of the differences observed. It may also be possible that the



**Figure 6. Direction-dependent strain fields of the tongue in the axial plane during respiration**
This is similar to the analysis in Fig. 5. It shows the deformed grids and the strain maps at different times during the respiratory cycle, superimposed on the tongue in the lower axial plane. The mandible and airway are shown with a white line. The three time points were selected based on data acquired from specific respiratory segments (see Methods). The strain maps are placed directly on top of the airway. The middle row of images represents tissue strain in the lateral direction and the lower row represents tissue strain in the anteroposterior direction. Tissue has zero strain at end-inspiration. Movement of the tongue was slightly asymmetric, giving rise to asymmetric strain patterns.

points tracked in the lateral walls and in the genioglossus are relatively stationary, while more superficial points on the airway wall move more to give rise to larger changes in airway calibre. Finally, as the mid-sagittal region of the genioglossus elongates posteriorly during expiration, this may open up airway regions to the side of the genioglossus, due to lateral narrowing of the genioglossus, since it acts as a hydrostat, as shown in the strain maps. This may contribute to the additional airway cross-sectional area reported during expiration (Schwab *et al.* 1993). By using fibre-optic endoscopy, Morrell & Badr (1998) measured changes in cross-sectional area at the level of the soft palate during wakefulness and sleep in normal and mild sleep apnoea patients. They showed that in wakefulness, there was little cross-sectional area change in this location, which is consistent with our findings of little tongue displacement in this region. Future studies using the current technique will elucidate the tongue motion during sleep.

In summary, this is the first study to examine how the human tongue and nearby structures deform to ensure airway patency during quiet breathing. It suggests that while patterns of local movement vary between subjects, there is anterior movement of the genioglossus muscle at the level of the epiglottis during inspiration with limited movement in nearby tissues including the geniohyoid.

## References

Amis TC, O'Neill N & Wheatley JR (1999). Oral airway flow dynamics in healthy humans. *J Physiol* **515**, 293–298.

Armstrong JJ, Leigh MS, Sampson DD, Walsh JH, Hillman DR & Eastwood PR (2006). Quantitative upper airway imaging with anatomic optical coherence tomography. *Am J Respir Crit Care Med* **173**, 226–233.

Bailey EF, Huang YH & Fregosi RF (2006). Anatomic consequences of intrinsic tongue muscle activation. *J Appl Physiol* **101**, 1377–1385.

Berry RB, White DP, Roper J, Pillar G, Fogel RB, Stanchina M & Malhotra A (2003). Awake negative pressure reflex response of the genioglossus in OSA patients and normal subjects. *J Appl Physiol* **94**, 1875–1882.

Brennick MJ, Gefter WB & Margulies SS (2007). Mechanical effects of genioglossus muscle stimulation on the pharyngeal airway by MRI in cats. *Respir Physiol Neurobiol* **156**, 154–164.

Brennick MJ, Pickup S, Dougherty L, Cater JR & Kuna ST (2004). Pharyngeal airway wall mechanics using tagged magnetic resonance imaging during medial hypoglossal nerve stimulation in rats. *J Physiol* **561**, 597–610.

Brennick MJ, Trouard TP, Gmitro AF & Fregosi RF (2001). MRI study of pharyngeal airway changes during stimulation of the hypoglossal nerve branches in rats. *J Appl Physiol* **90**, 1373–1384.

Brown IG, Zamel N & Hoffstein V (1986). Pharyngeal cross-sectional area in normal men and women. *J Appl Physiol* **61**, 890–895.

Cheng S, Gandevia S & Bilston L (2007). Deformation of the upper airway musculature during quiet breathing in humans. *Eur Respir J* **30**, 521.

Eastwood PR, Allison GT, Shepherd KL, Szollosi I & Hillman DR (2003). Heterogeneous activity of the human genioglossus muscle assessed by multiple bipolar fine-wire electrodes. *J Appl Physiol* **94**, 1849–1858.

Fogel RB, Trinder J, Malhotra A, Stanchina M, Edwards JK, Schory KE & White DP (2003). Within-breath control of genioglossal muscle activation in humans: effect of sleep-wake state. *J Physiol* **550**, 899–910.

Fregosi RF (2008). Influence of tongue muscle contraction and dynamic airway pressure on velopharyngeal volume in the rat. *J Appl Physiol* **104**, 682–693.

Gilbert RJ, Napadow VJ, Gaige TA & Wedeen VJ (2007). Anatomical basis of lingual hydrostatic deformation. *J Exp Biol* **210**, 4069–4082.

Horner RL, Innes JA, Murphy K & Guz A (1991). Evidence for reflex upper airway dilator muscle activation by sudden negative airway pressure in man. *J Physiol* **436**, 15–29.

Hudgel DW, Devadatta P & Hamilton H (1993). Pattern of breathing and upper airway mechanics during wakefulness and sleep in healthy elderly humans. *J Appl Physiol* **74**, 2198–2204.

Innes JA, Morrell MJ, Kobayashi I, Hamilton RD & Guz A (1995). Central and reflex neural control of genioglossus in subjects who underwent laryngectomy. *J Appl Physiol* **78**, 2180–2186.

Kier WM, Smith KK & Miyan JA (1989). Trunks, tongues and tentacles: moving with skeletons of muscle. *Am Sci* **77**, 22–35.

Kuna ST (2004). Regional effects of selective pharyngeal muscle activation on airway shape. *Am J Respir Crit Care Med* **169**, 1063–1069.

Malhotra A, Pillar G, Fogel RB, Beauregard J, Edwards JK, Slamowitz DI, Shea SA & White DP (2000). Genioglossal but not palatal muscle activity relates closely to pharyngeal pressure. *Am J Respir Crit Care Med* **162**, 1058–1062.

Malhotra A, Pillar G, Fogel RB, Edwards JK, Ayas N, Akahoshi T, Hess D & White DP (2002). Pharyngeal pressure and flow effects on genioglossus activation in normal subjects. *Am J Respir Crit Care Med* **165**, 71–77.

Mathew OP, Abu-Osba YK & Thach BT (1982). Influence of upper airway pressure changes on genioglossus muscle respiratory activity. *J Appl Physiol* **52**, 438–444.

Mezzanotte WS, Tangel DJ & White DP (1992*a*). Waking genioglossal electromyogram in sleep apnea patients versus normal controls (a neuromuscular compensatory mechanism). *J Clin Invest* **89**, 1571–1579.

Mezzanotte WS, Tangel DJ & White DP (1992*b*). Mechanisms of control of alae nasi muscle activity. *J Appl Physiol* **72**, 925–933.

Morrell MJ & Badr MS (1998). Effects of NREM sleep on dynamic within-breath changes in upper airway patency in humans. *J Appl Physiol* **84**, 190–199.

Napadow VJ, Chen Q, Wedeen VJ & Gilbert RJ (1999*a*). Intramural mechanics of the human tongue in association with physiological deformations. *J Biomech* **32**, 1–12.

Napadow VJ, Chen Q, Wedeen VJ & Gilbert RJ (1999*b*). Biomechanical basis for lingual muscular deformation during swallowing. *Am J Physiol Gastrointest Liver Physiol* **277**, G695–G701.

Napadow VJ, Mai V, Bankier A, Gilbert RJ, Edelman R & Chen Q (2001). Determination of regional pulmonary parenchymal strain during normal respiration using spin inversion tagged magnetization MRI. *J Magn Reson Imaging* **13**, 467–474.

Osman NF, Kerwin WS, McVeigh ER & Prince JL (1999). Cardiac motion tracking using CINE harmonic phase (HARP) magnetic resonance imaging. *Magn Reson Med* **42**, 1048–1060.

Osman NF, McVeigh ER & Prince JL (2000). Imaging heart motion using harmonic phase MRI. *IEEE Trans Med Imaging* **19**, 186–202.

Parthasarathy V, Prince JL, Stone M, Murano EZ & Nessaiver M (2007). Measuring tongue motion from tagged cine-MRI using harmonic phase (HARP) processing. *J Acoust Soc Am* **121**, 491–504.

Pierce R, White D, Malhotra A, Edwards JK, Kleverlaan D, Palmer L & Trinder J (2007). Upper airway collapsibility, dilator muscle activation and resistance in sleep apnoea. *Eur Respir J* **30**, 345–353.

Pillar G, Fogel RB, Malhotra A, Beauregard J, Edwards JK, Shea SA & White DP (2001). Genioglossal inspiratory activation: central respiratory vs mechanoreceptive influences. *Respir Physiol* **127**, 23–38.

Prince JL & McVeigh ER (1992). Motion estimation from tagged MR image sequences. *IEEE Trans Med Imaging* **11**, 238–249.

Saboisky JP, Butler JE, Fogel RB, Taylor JL, Trinder JA, White DP & Gandevia SC (2006). Tonic and phasic respiratory drives to human genioglossus motoneurons during breathing. *J Neurophysiol* **95**, 2213–2221.

Saboisky JP, Butler JE, Walsh LD & Gandevia SC (2007). New display of the timing and firing frequency of single motor units. *J Neurosci Methods* **162**, 287–292.

Sauerland EK & Harper RM (1976). The human tongue during sleep: electromyographic activity of the genioglossus muscle. *Exp Neurol* **51**, 160–170.

Schwab RJ, Gefter WB, Pack AI & Hoffman EA (1993). Dynamic imaging of the upper airway during respiration in normal subjects. *J Appl Physiol* **74**, 1504–1514.

Strohl KP, Hensley MJ, Hallett M, Saunders NA & Ingram RH Jr (1980). Activation of upper airway muscles before onset of inspiration in normal humans. *J Appl Physiol* **49**, 638–642.

Takemoto H (2001). Morphological analyses of the human tongue musculature for three-dimensional modeling. *J Speech Lang Hear Res* **44**, 95–107.

Tangel DJ, Mezzanotte WS & White DP (1995). Respiratory-related control of palatoglossus and levator palatini muscle activity. *J Appl Physiol* **78**, 680–688.

Tobin MJ, Chadha TS, Jenouri G, Birch SJ, Gazeroglu HB & Sackner MA (1983). Breathing patterns. 1. Normal subjects. *Chest* **84**, 202–205.

Trudo FJ, Gefter WB, Welch KC, Gupta KB, Maislin G & Schwab RJ (1998). State-related changes in upper airway caliber and surrounding soft-tissue structures in normal subjects. *Am J Respir Crit Care Med* **158**, 1259–1270.

Wheatley JR, Kelly WT, Tully A & Engel LA (1991). Pressure-diameter relationships of the upper airway in awake supine subjects. *J Appl Physiol* **70**, 2242–2251.

Worsnop C, Kay A, Kim Y, Trinder J & Pierce R (2000). Effect of age on sleep onset-related changes in respiratory pump and upper airway muscle function. *J Appl Physiol* **88**, 1831–1839.

Worsnop C, Kay A, Pierce R, Kim Y & Trinder J (1998). Activity of respiratory pump and upper airway muscles during sleep onset. *J Appl Physiol* **85**, 908–920.

Yokoba M, Hawes HG & Easton PA (2003). Geniohyoid muscle function in awake canines. *J Appl Physiol* **95**, 810–817.

## Acknowledgements

## Supplemental material

Online supplemental material for this paper can be accessed at: http://jp.physoc.org/cgi/content/full/jphysiol.2008.156430/DC1